Optical Characterization of CLPS Miniature Laser Retroreflector Arrays

Daniel R. Cremons[1], Xiaoli Sun[1], Zachary Denny[1], Shane W. Wake[1], Evan D. Hoffman[1], Erwan Mazarico[1], Edward C. Aaron[2], David E. Smith[3]

[1]NASA Goddard Space Flight Center, Greenbelt, MD 20771
[2]KBRwyle Technology Solutions, LLC, Lanham, MD 20706
[3]Massachusetts Institute of Technology, Cambridge, MA 02139

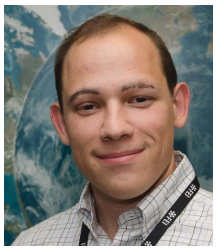

PRESENTED AT:

INTRODUCTION AND MOTIVATION

Laser retroreflector arrays (LRAs) consisting of corner cube retroreflectors (CCRs) can act as fiducial markers for decades of laser ranging on the Moon and other planetary bodies. Upcoming lunar lander missions from government space agencies and commercial partners offer a unique opportunity to support lunar science and exploration through the deployment of small LRAs on lander decks. Placement of an LRA on the deck of a lander or rover enables tracking with an orbital laser altimeter to a precision on the order of centimeters. When mounted alongside a suite of scientific instruments the LRA enables precise geolocation of those instruments in the lunar geodetic frame. Finally, optical markers such as LRAs can support precision autonomous navigation and landing regardless of lighting conditions, an especially valuable capability for lunar polar exploration where long shadows complicate terrain relative nagivation using imaging methods.

Array Design	Hemispherical
Array Diameter	5.11 cm
Array Height	1.65 cm
CCR Clear Aperture	1.27 cm
Number of CCRs	8
Mass	20 g

Figure 1. LRALL after integration with SpaceIL Beresheet lander deck in Nov. 2018.

Here we present the optical characterization results of Laser Retroreflector Arrays for Lunar Landers (LRALL) developed under the Commercial Lunar Payload Services (CLPS) program [1,2]. LRALL is a passive optical instrument designed to provide a high-gain target which can be ranged to with a lunar-orbiting laser altimeter from any azimuth angle above 30° in elevation from the mounting plane. These low-mass, small instruments (Figure 1) were designed and tested for decades of lifetime on the lunar surface, including radiation testing to 19 Mrad (Si). The arrays can be ranged to from orbiting lunar spacecraft such as LRO or Gateway provided there is a laser altimeter onboard. They will also act as beacons for lidars on future landers making return missions to the CLPS lander locations (*e.g.,* to retrieve samples collected by the original CLPS lander). LRALL can operate over the entire lunar day and night and is completely passive; the arrays require no power, communication, or thermal control. LRALL units are manifested on upcoming CLPS missions, including Peregrine Mission 1 (Astorbotic), IM-1 (Intuitive Machines), and Masten Mission 1 (Masten Space). The objective of this poster presentation is to provide detailed optical characteristics of the LRA for future lunar lidar ranging to the LRAs.

LASER RETROREFLECTOR ARRAY OPTICAL TESTING PROGRAM

Our optical test program baseline was derived from the qualification of retroreflector arrays for satellite laser ranging (SLR) [3,4]. However, we also tested optical performance at both visible and near infrared wavelengths, tracked performance over the lunar temperature range, and performed a detailed study of the interference effects of multiple-cube returns.

The primary optical figures of merit for the CCRs are the surface flatness and the dihedral angle error (DAE), or the deviation from 90° of the angles between the facets of the prism. All 13 LRALL units tested met the design specification of surface flatness of 1/10 λ at 532 nm and an average DAE within ± 0.5 arcsec.

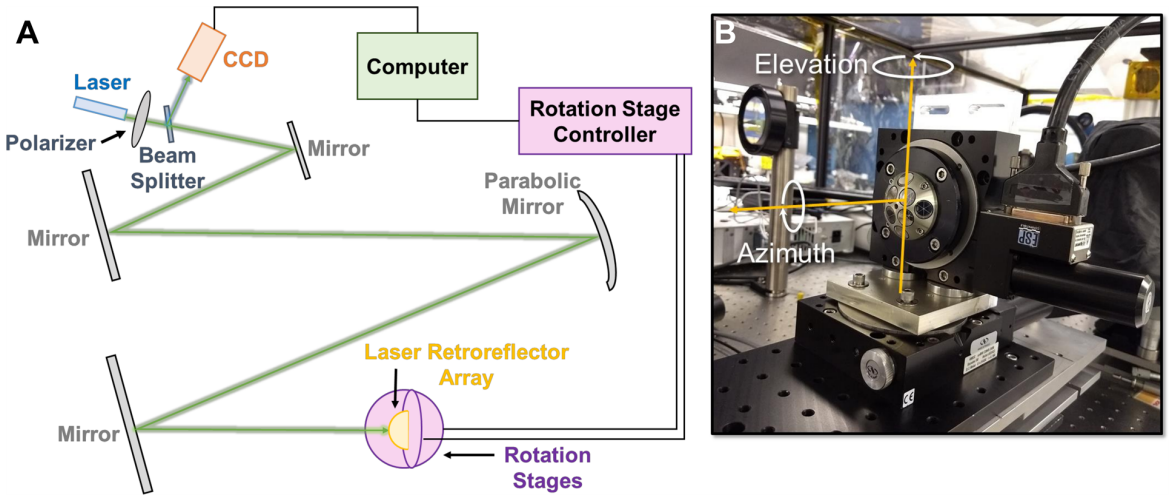

Figure 2. Optical test setup for visible and infrared optical cross section measurements and cube inteference study.

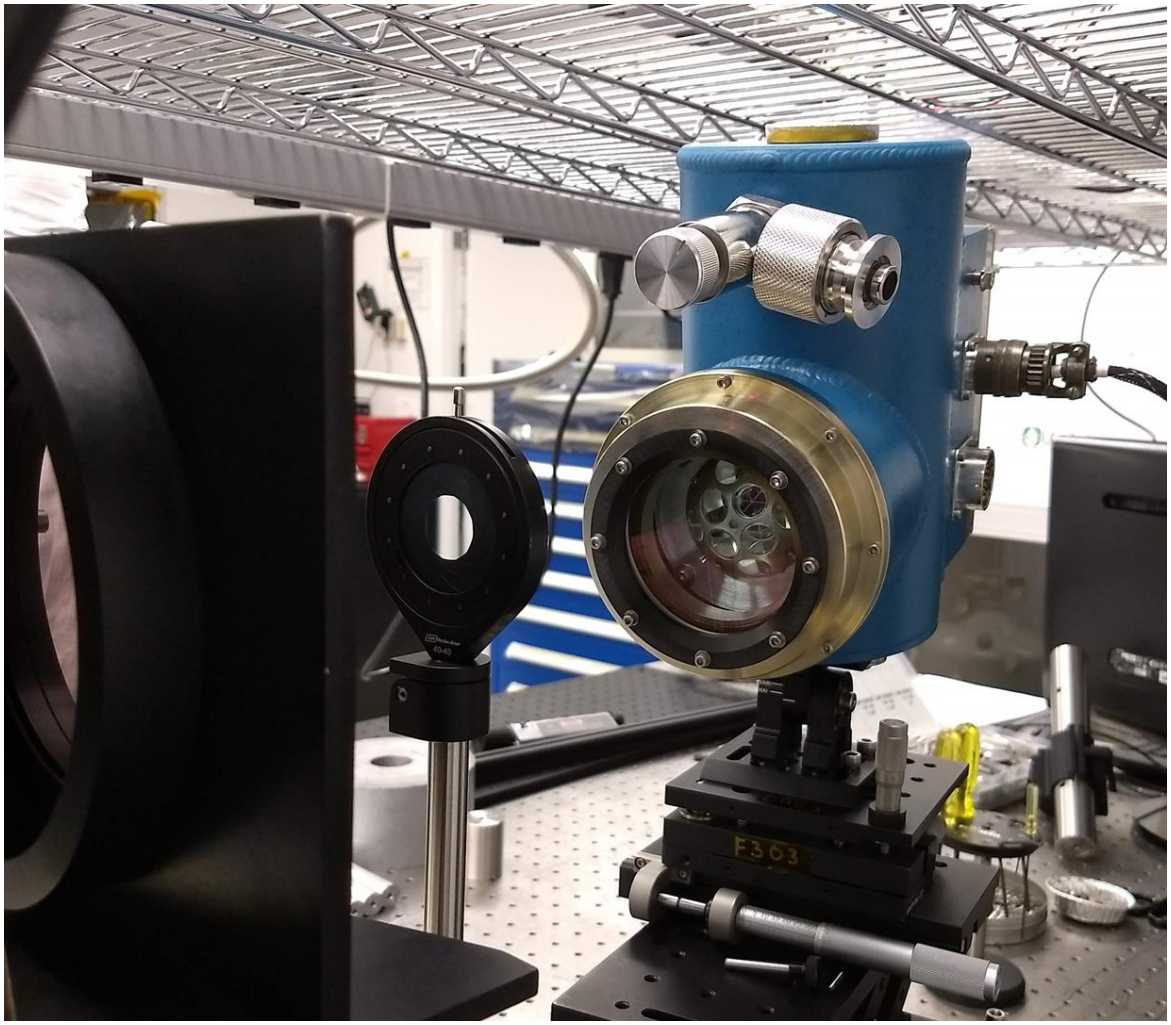

Figure 3. Experimental test setup for cryogenic interferometer tests. The window of the Zygo Verifire inteferometer can be seen in the left foreground. The iris was used to only illuminate a single CCR in the array to remove interference effects. The liquid nitrogen vacuum Dewar was tilted to ensure the CCR front face was normal to the interferometer beam.

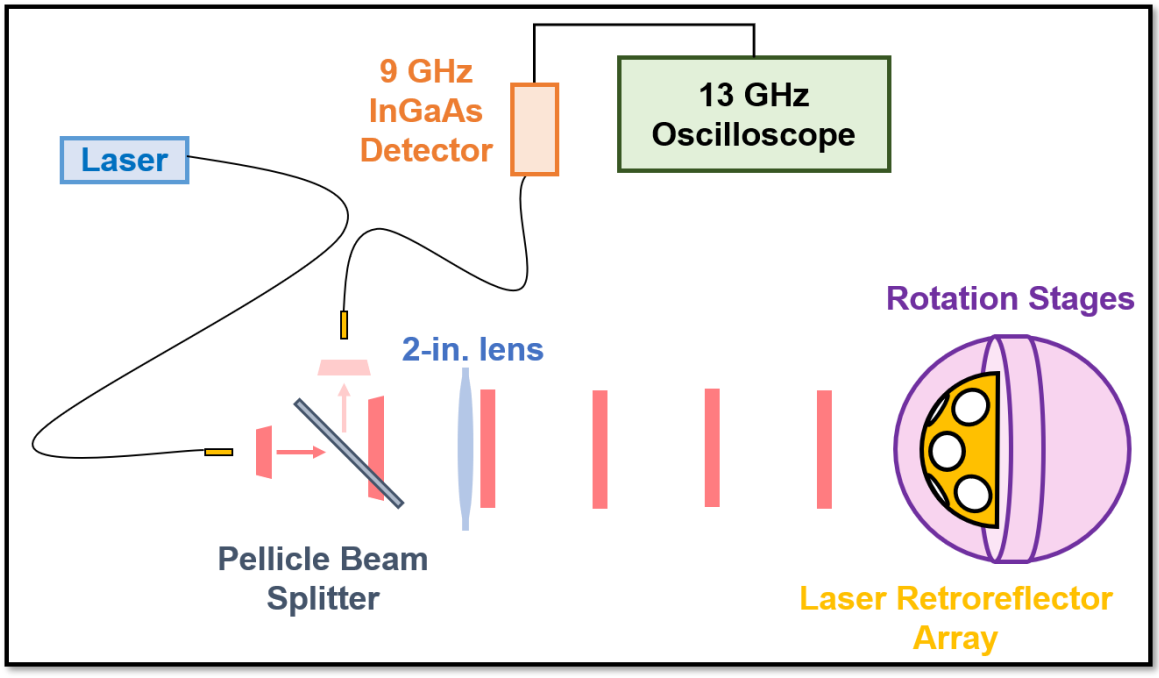

Figure 4. Experimental test setup for pulse waveform tests.

FAR FIELD DIFFRACTION PATTERN AND OPTICAL CROSS SECTION MEASUREMENTS

A far-field diffraction pattern (FFDP) is the spatial and intensity distribution of light returned to an interrogating laser source from an illuminated CCR under Fraunhofer conditions (i.e., the distance from the source to the CCR is much greater than the aperture diameter). We performed a series of optical tests of the LRALL instruments to measure the FFDPs over a broad range of incident angles (Figure 5) at both 532 nm and 1064 nm. By comparing the quantiative signal from these FFDPs to the signal from a same-sized circular mirror with a calibrated reflectance, the optical cross sections were calcluated. The peak optical cross section occurred at 70° in elevation in conjuection with the inner ring of CCRs, with a second maximum corresponding to the the second ring of CCRs.

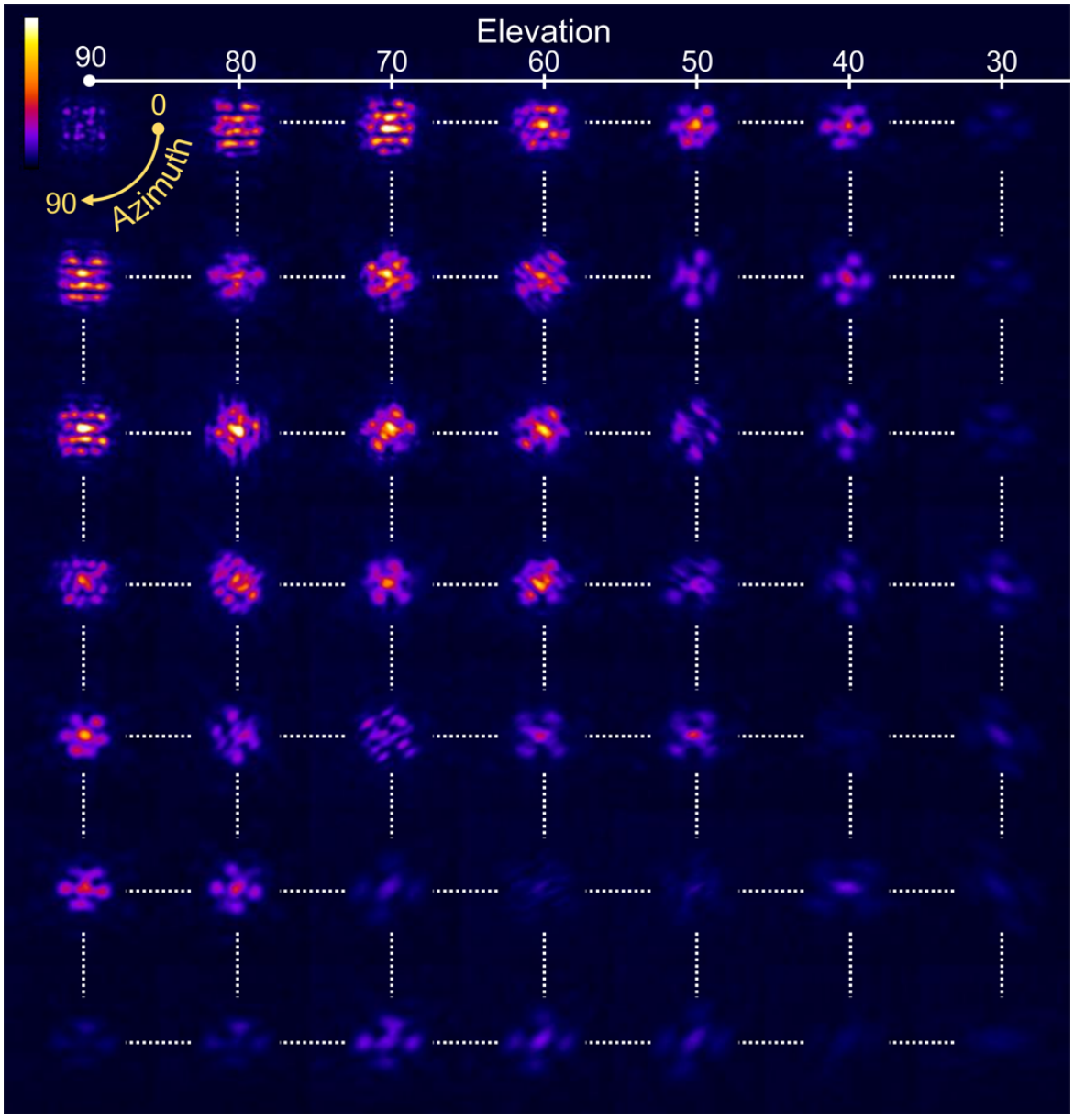

Figure 5. Montage of FFDPs from LRA in equirectangular projection. The color scale is shown in the upper left and corresponds to relative optical cross section, with warmer colors corresponding to higher optical return. FFDPs were all obtained under identical imaging and illumination conditions.

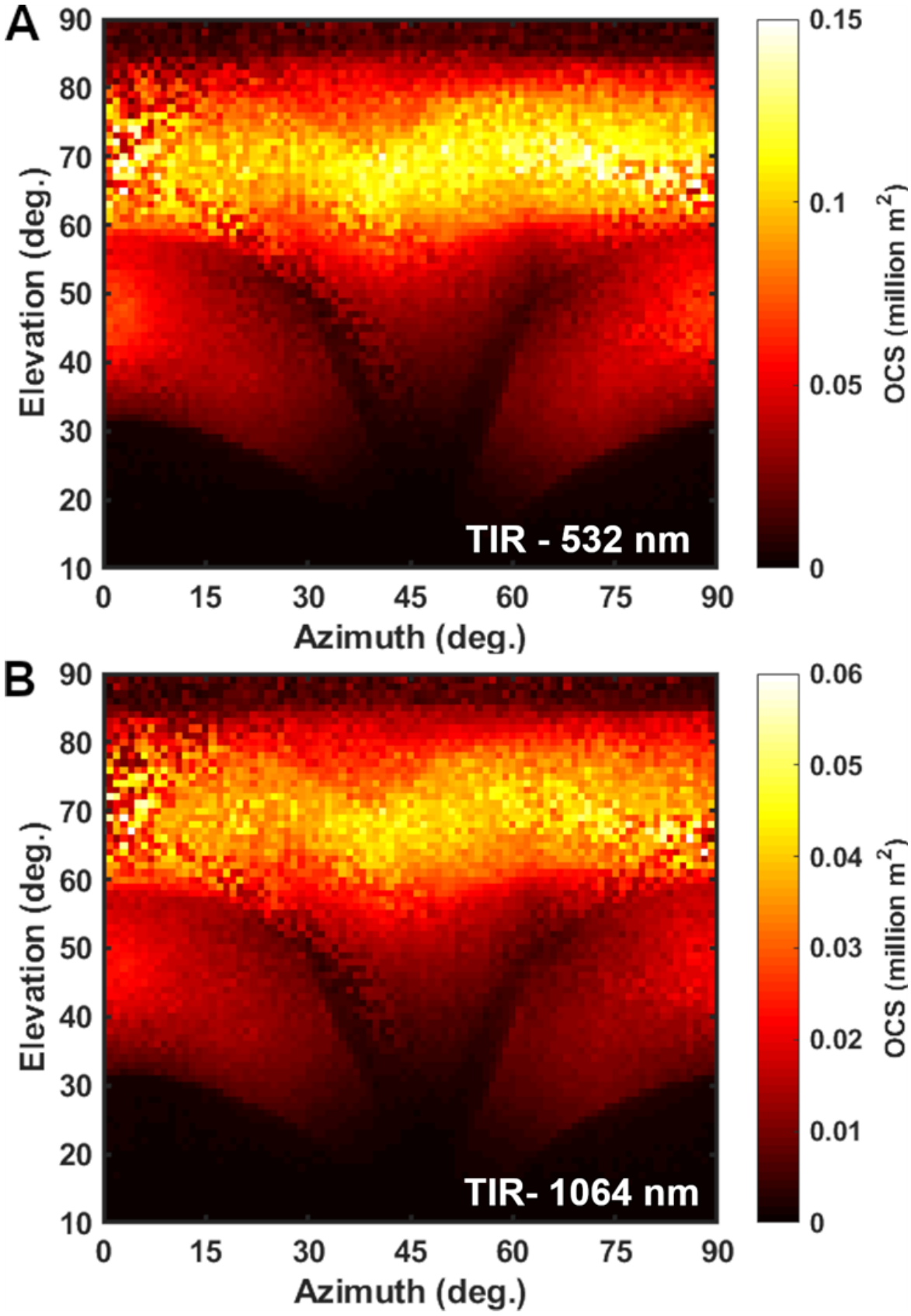

Figure 6. Map of optical return from the retroreflector array as a function of incident angle for LRALL. (A) Map created from FFDPs using 532-nm illumination. (B) Map created from FFDPs using 1064-nm illumination. The color scales correspond to the optical cross section under lunar ranging conditions (50 km orbit) with warmer, lighter colors denoting higher optical return. Elevation and Azimuth angles refer to terminology defined in Figure 2. Far-field diffraction patterns were obtained in one-degree intervals in both elevation and azimuth for the ranges shown; each pixel of the map represents a distinct far-field diffraction

pattern from which the optical cross section was extracted. The pixel-to-pixel variation is real and is a result of sampling a complex interference pattern.

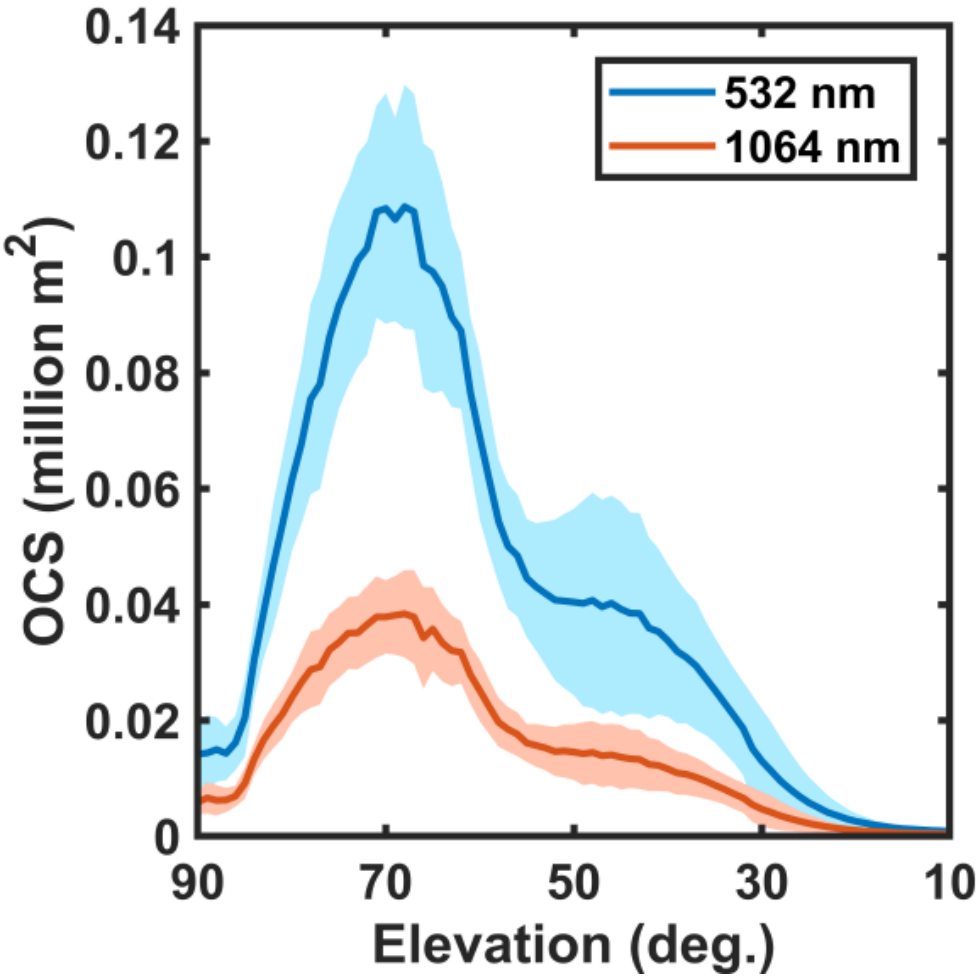

Figure 7. Azimuthally-averaged optical performance of LRALL as a function of elevation angle. The dark blue and dark red lines denote the azimuthal average value for each elevation, while the light blue and light red shaded regions denote the 1σ variance at each elevation from the population of all azimuth angles.

CRYOGENIC INTERFEROMETER AND PULSE WAVEFORM TEST RESULTS

Temperature Test Results

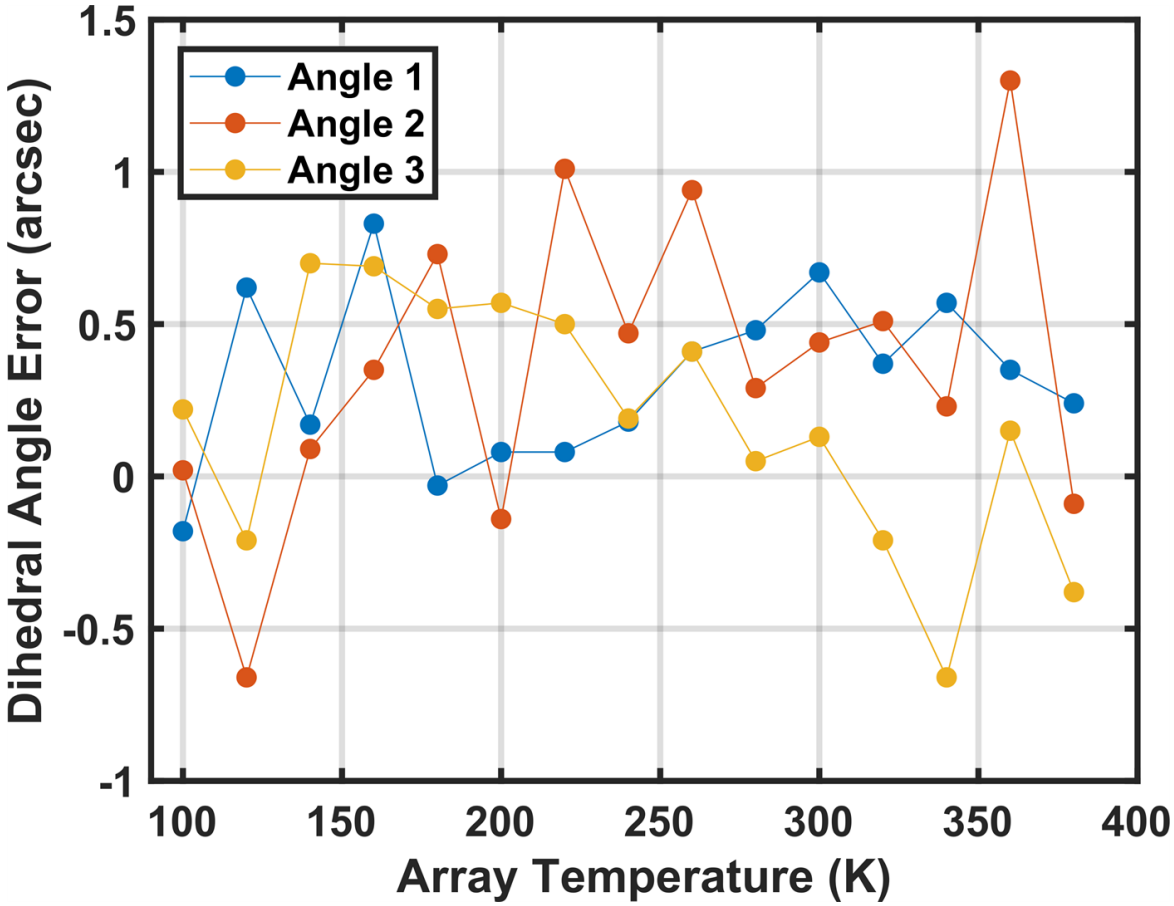

Figure 8. Measured dihedral angle errors of a total internal reflection CCR over the expected lunar temperature range.

The thermal extremes experienced on the lunar surface over the course of the diurnal cycle – from 95 K to 385 K at the equator [5] – can induce thermal gradients in both coated and total internal reflection CCRs [6], though metal-coated CCRs are more susceptible to this effect. This effect can lead to a reduced optical cross-section for gradients as small as 4 K from the front surface to the rear vertex of the CCR [7]. We mounted the LRA in a customized vacuum Dewar and chilled the array to cryogenic temperatures. Step heating from cryogenic temperatures was performed via a 100-W cartridge heater fixed to the rear of the LRA mounting plate. DAE measurements were obtained from 100 K to 380 K in 20 K steps. We observed small variations in the DAEs over the lunar surface temperature range, and the three angles in the CCR exhibited different trends from one another (Figure 8). For the entire observed temperature range, all three DAEs varied over a range near the tolerance of the CCRs. This suggests that no strong axial or radial thermal gradients were present in the 1.27-cm CCRs that would impact optical performance under test conditions. On the lunar surface solar illumination can induce thermal gradients in the CCRs due to thermal breakthrough (loss of total internal reflection) of the TIR CCRs at angles above ~17° and via conduction through the aluminum shell. However, the small size of the CCRs in LRALL (1/10 the area of the Apollo CCRs) should reduce the magnitude of thermal gradients while on the lunar lander deck.

Pulse Waveform Test Results

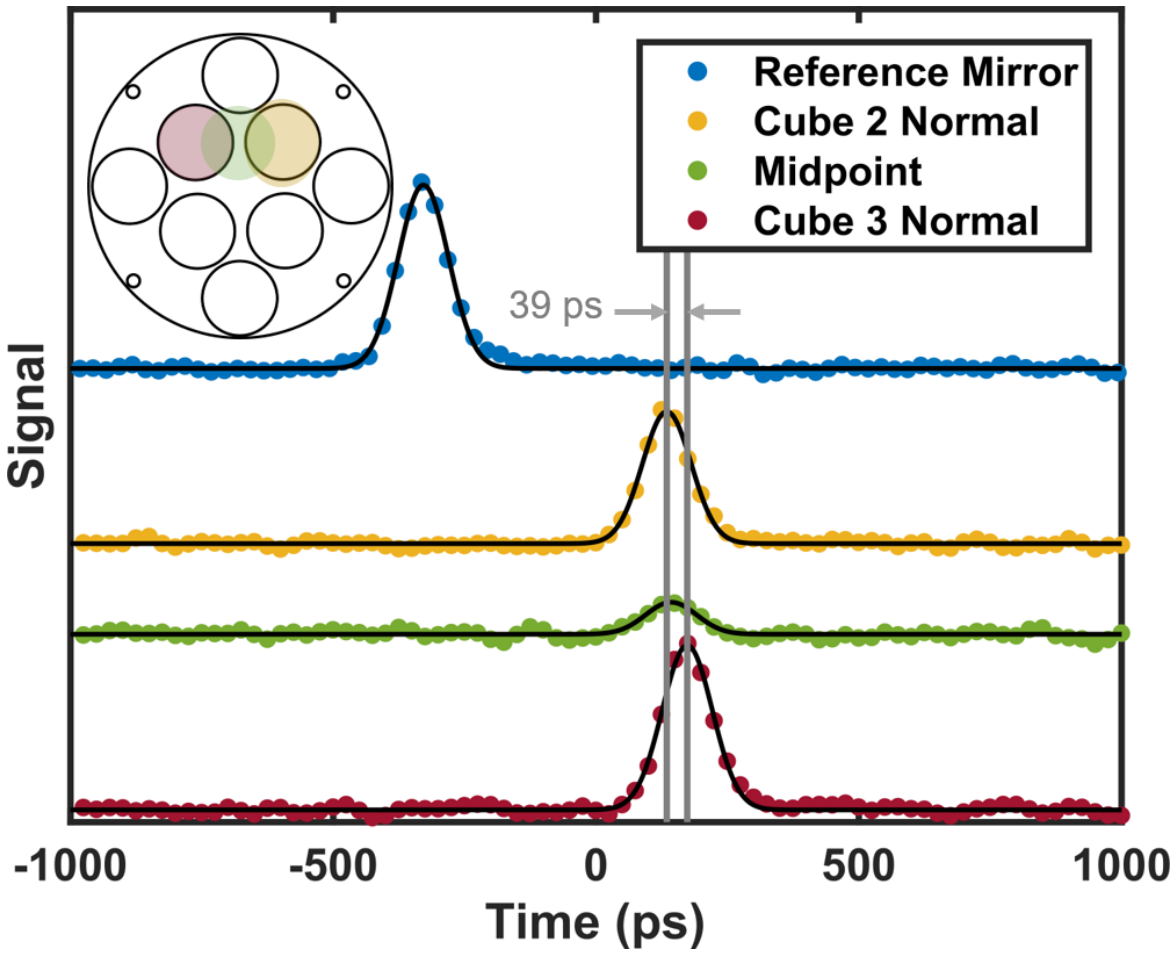

Figure 9.

We used a 1064-nm fiber-coupled, pulsed laser source to measure the pulsed laser return from the LRA to check for pulse spreading or distortion by the array as well as to test for range changes as a function of incident angle which could limit the range measurement resolution. The measured pulsewidth was 48 ps (Gaussian RMS width) from the reference mirror, including the effects of the photodiode and oscilloscope. We captured the return waveforms at three laser incidence angles, as shown in Figure 9. The laser pulse shape was unchanged by the array as measured on the system described here, with a Gaussian RMS width of 46 to 49 ps compared to 48 ps when using a reference mirror. The delay time between cubes as measured from the gaussian centroid positions was 39 ps, which corresponds to 6 mm in range offset.

REFERENCES

[1] Sun X. et al. (2019) Appl. Opt., 58, 9259-9266.

[2] Cremons D. R. et al. (2020) Appl. Opt., 59, 5020-5031.

[3] Degnan, J. J. (1993) Contributions to Space Geodesy and Geodynamics: Technology, 25, 133-162.

[4] Minott P. O. et al. (1993) Prelaunch optical characterization of the laser geodynamic satellite (LAGEOS 2).

[5] Vasavada J. L. et al. (2012) J. Geophys. Res.: Planets, 117, E12.

[6] Murphy T. W. et al. (2010) Icarus, 208, 31-35.

[7] Goodrow S. D. and Murphy T. W. (2012) Appl. Opt., 51, 8793-8799.